Far-infrared Alfven waves in graphite

1989 J. Phys.: Condens. Matter 1 6829

(http://iopscience.iop.org/0953-8984/1/38/007)

J. Phys.: Condens. Matter 1 (1989) 6829–6834. Printed in the UK

Far-infrared Alfvén waves in graphite

W R Datars and A Weingartshofer
Department of Physics, McMaster University Hamilton, Ontario, Canada, L8S 4M1

Received 30 January 1989, in final form 8 June 1989

Abstract. Alfvén-wave propagation in single-crystal graphite has been studied at 4.2 K with wavelengths of 392.5, 433 and 512.5 μm in magnetic fields up to 8.5 T applied along the c axis in the Faraday geometry. The mass density function obtained from the magnetic field dependence of interference maxima is in excellent agreement with the predicted value from the parameters of graphite. The amplitude of the propagating wave is larger with the circular polarisation of the infrared set to sense holes than it is to sense electrons and the amplitude is reduced when the hole Landau levels coincide with the Fermi surface. The propagating wave has a higher amplitude for the hole polarisation at a given magnetic field because the holes have a smaller mass than the electrons but the dispersion of the propagating wave is given by the linear wave approximation for Alfvén waves.

1. Introduction

Alfvén waves can propagate in a solid state plasma having equal numbers of electrons and holes in the presence of a magnetic field when the cyclotron frequency is much greater than the frequency of the applied radiation (Buchsbaum and Galt 1961). They have been studied extensively in bismuth at microwave frequencies (Isaacson and Williams 1969, and references therein). It has been shown that graphite, which is also a semi-metal, can also support Alfvén wave propagation at a frequency of 35 GHz (Surma *et al* 1964, Furdyna and Krauss 1971). Alfvén waves are one of the magneto-plasma effects which have been reviewed by Palik and Furdyna (1970).

In the present paper, we investigate the properties of Alfvén waves with far-infrared frequencies produced by a far-infrared laser optically pumped by a CO_2 laser. Circular polarisation of the radiation and magnetic fields up to 8.5 T allowed a complete study in graphite.

An electromagnetic wave in a plasma is described by the equation

$$\nabla^2 \boldsymbol{E} + (\omega^2/c^2)\boldsymbol{\varepsilon}(\omega, \boldsymbol{k}) \cdot \boldsymbol{E} = 0 \tag{1}$$

where $\varepsilon(\omega, k)$ is the complex dielectric function of the medium in the presence of a magnetic field. Alfvén waves can exist under the conditions that

$$\omega_p^2/\varepsilon_l \gg \omega_c^2 \gg \omega^2 \gg \nu_{\text{eff}}^2 \tag{2}$$

where ω and ν_{eff} are the far-infrared frequency and the effective carrier scattering frequency, respectively. ω_p and ω_c are the plasma and cyclotron frequencies of each carrier, respectively, and ε_l is the high-frequency dielectric constant associated with electronic, interband transitions. The dielectric function for propagation of an Alfvén wave along the magnetic field direction (the z direction) in the Faraday geometry is

$$\varepsilon_{xx} = (M^2 c/B^2)(1 + \mathrm{i}\nu_{\mathrm{eff}}/\omega) \tag{3}$$

where

$$M = [4\pi n(m_{\mathrm{e}} + m_{\mathrm{h}})]^{1/2} \tag{4}$$

is the effective mass density of the medium and

$$\nu_{\mathrm{eff}} = (\nu_{\mathrm{e}} m_{\mathrm{e}} + \nu_{\mathrm{h}} m_{\mathrm{h}})/(m_{\mathrm{e}} + m_{\mathrm{h}}) = (4\pi B^2/c^2 M^2)\sigma_{xx}(0, \omega_{\mathrm{c}}) \tag{5}$$

is the effective scattering rate. Here, m_{e} and m_{h} are the masses of the electrons and holes, respectively, with a carrier density n and $\sigma_{xx}(0, \omega_{\mathrm{c}})$ is the DC conductivity.

The propagation vector is

$$\boldsymbol{k} = \omega M/B + \mathrm{i}(M/2B)\nu_{\mathrm{eff}}. \tag{6}$$

Propagation takes place when the dielectric function is real and positive with an Alfvén velocity

$$v_{\mathrm{A}} = B/M. \tag{7}$$

There are constructive maxima between the propagating wave through the sample of thickness d and the radiation in free space with a wavelength λ_0 when

$$N\lambda_0 = \eta d \tag{8}$$

when η is the refractive index $= c/v_{\mathrm{A}}$. Therefore

$$N\lambda_0 = (cM/B)d \tag{9}$$

from which a plot of the integer N versus B^{-1} yields the mass density of the medium.

A Fabry–Perot interference pattern from multi-reflections in the sample for which $N\lambda_0 = 2nd$ is satisfied rather than equation (8) also has to be considered. However, it did not exist in bismuth although it was assumed to take place in early work (Isaacson and Williams 1969) and it did not occur in graphite at microwave frequencies (Furdyna and Krauss 1971). Equation (8) also describes the interference pattern in this experiment.

2. Experiment

The radiation was produced with a far-infrared (FIR) optically pumped laser. The optical pump was a CO_2 laser operating with a flowing mixture of 13% CO_2, 22% N_2 and 65% He at a pressure of about 15 Torr. The wavelength range of the laser was 9–11 μm and typical power output was 20 W. The beam from the laser passed through a CdS circular polariser before entering the FIR cavity to reduce the reflected beam back into the CO_2 laser which interferes with the operation of the laser. The CO_2 laser beam was reflected through 180° before entering the FIR cavity which was a gold-plated, brass light guide 122 cm long and 5 cm in diameter containing either methyl alcohol (CH_3OH) or formic acid (HCOOH). The typical power of the FIR output was between 5 and 15 mW.

Passive stability was improved by connecting the FIR extraction and injection boxes with invar rods and vibration stability was supplied by a table consisting of a hardwood box containing 1000 kg of sand. In addition, there was an electronic feedback loop to provide long-term stabilisation. The electrode voltage of the CO_2 laser was applied as a square wave with a frequency of 24.5 Hz. Then, approximately 50% of the FIR laser output was directed by a beam splitter to a pyroelectric detector. Its output was phase-sensitive detected by a lock-in amplifier and was used to adjust the current of the CO_2 discharge. This stabilisation achieved noise levels as low as 0.05% and the typical noise level for extended periods of time was 0.1–0.2% of the total FIR power. The FIR radiation passing through the beam splitter was directed to the sample by a brass light pipe.

A polariser employing the method of Schaber and Doezema (1978) was above the sample. It consisted of a mylar-mesh, linear polariser properly oriented above a quartz quarter-wave plate to add the slow and fast modes in the plate to form circular polarisation. The light from the sample was reflected directly to a gallium-doped germanium detector. Two quarter-wave plates designed for 119 μm and 430 μm were used. The degree of polarisation was determined from the low-field cyclotron resonance, which is clearly different for the polarisations sensitive to electrons and holes (Doezema *et al* 1979). The polarisation sense was changed by changing the direction of the magnetic field. Use of the 119 μm polariser posed no problems since the polarisation of the 118.8 μm laser line was not affected greatly by small misalignments of the polariser. However, the alignment of the 430 μm polariser had to be more precise and the circular polarisation of the 392.5 and 433 μm lines was not total. It was sufficient to distinguish between hole and electron polarisation with a ratio of 3 : 1.

The wavelengths (frequencies) from formic acid that were used are 118.8 μm (2525 GHz), 392.5 μm (764 GHz), 433.0 μm (693 GHz) and 512.5 μm (585 GHz). The magnetic field was provided by a 8.5 T superconducting solenoid and was directed along the graphite c axis. Highly oriented pyrolytic graphite (HOPG) samples were tested but natural single crystals from a quarry near Harrisville, NY were used in all the experiments.

3. Results and discussion

The interferogram from Alfvén wave propagation in single-crystal graphite is shown in figure 1 for a wavelength of 433 μm with hole polarisation and a sample thickness of 330 μm. The data were taken at 4.2 K and no difference was noted when the temperature was lowered to 1.5 K. There is an interference pattern between 3.0 and 8.5 T due to the magnetic field dependence of the wave velocity. In addition, there is a minimum at 4.8 T from a dielectric anomaly. It occurs when the dielectric constant goes through zero.

The magnetic field of the dielectric anomaly changes with frequency and is 5.5 T at 763 GHz (wavelength 393 μm) and 4.3 T at 583 GHz (512.5 μM).

The dispersion of the reciprocal fields of the maxima of the reflected signal shown in figure 2 confirms the Alfvén wave nature of the propagation. The maximum at the highest field is assigned $N = 1$ since the absolute value of N is not known. The effective mass density derived from the slope of the plot according to equation (9) is 5.7×10^{-5} $(\mathrm{g\,cm^{-3}})^{1/2}$. The effective mass densities derived in a similar way with the same sample at the wavelengths of 512.5 μm and 393 μm are 5.8×10^{-5} $(\mathrm{g\,cm^{-3}})^{1/2}$ and 5.4×10^{-5} $(\mathrm{g\,cm^{-3}})^{1/2}$ respectively. The average mass density from the three measurements is 5.6 ± 0.2 $(\mathrm{g\,cm^{-3}})^{1/2}$. This value is in agreement with the predicted value for graphite of 5.65×10^{-5} $(\mathrm{g\,cm^{-3}})^{1/2}$ obtained using a charge density of electrons and holes of $2.9 \times 10^{18}\ \mathrm{cm^{-3}}$ (McClure 1958) and cyclotron masses of electrons and holes of $0.057m_0$

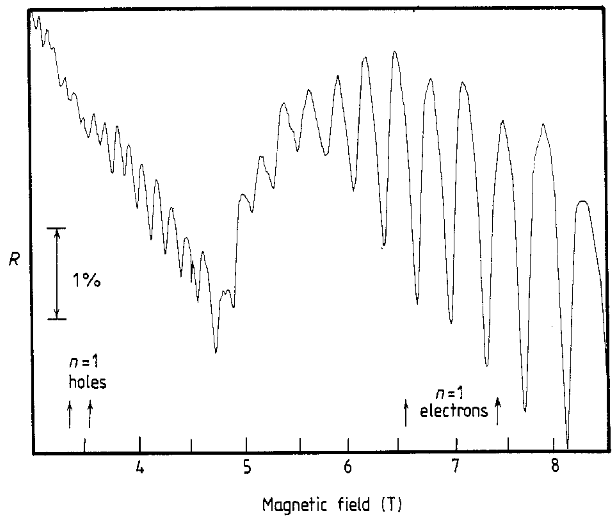

Figure 1. The reflected signal for a FIR wavelength of 433 μm with hole polarisation of single-crystal graphite with a thickness of 330 μm as a function of magnetic field from 3.0 to 8.5 T. The arrows show the magnetic fields of the spin-split minima in the magnetoresistance for $n = 1$ electrons and $n = 1$ holes.

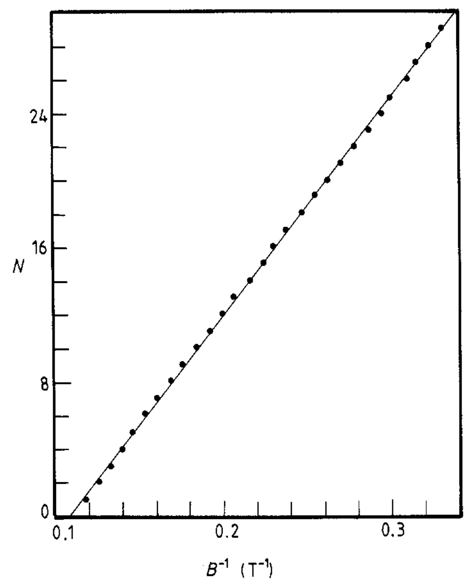

Figure 2. Integer N versus reciprocal field of Alfvén wave interference maxima for a far-infrared wavelength of 433 μm. The solid line is a linear least squares fit to the data.

and $0.039m_0$ (Soule *et al* 1964). However, the predicted value is in disagreement with the average mass density of $(4.8 \times 10^{-5})^{1/2}$ (g cm^{-3})$^{1/2}$ measured by Furdyna and Krauss (1971) at a microwave frequency of 35 GHz with a sample thickness similar to our sample thickness. Thus, the discrepancy between theory and experiment reported in the early work is removed at far-infrared wavelengths. This probably results from the fact that the absolute value of N in equation (8) is larger with the use of the smaller far-infrared wavelength.

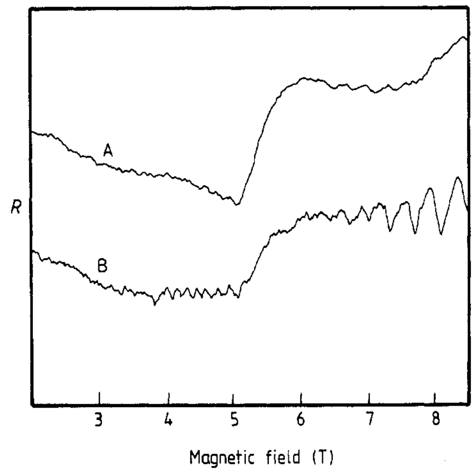

Figure 3. The reflected signal from single-crystal graphite as a function of magnetic field with the direction relative to the direction of the circular polarisation at a wavelength of 393.5 μm set to sense (A) electrons (B) holes.

Alfvén waves were not observed at a wavelength of 118.8 μm in magnetic fields up to 8.5 T. This is because the maximum field was not sufficiently above the fundamental electron cyclotron resonance field of 5.8 T for the propagation to occur. Also Alfvén wave propagation in well annealed HOPG samples was not observed at any far-infrared wavelength although cyclotron resonance of electrons and holes was clearly in evidence. This is surprising because propagation in pyrolytic graphite was observed by Furdyna and Krauss at a frequency of 35 GHz. Perhaps the lack of order along the *c* axis of HOPG randomises the phase of the wave at far-infrared wavelengths.

Circular polarisation experiments with a polarisation ratio of 3 : 1 revealed clear differences in the reflected signal for electron-sense and hole-sense polarisation as shown in figure 3 for a wavelength of 393.5 μm. Similar results were obtained for 433 μm. The dielectric anomaly is twice as large for electron polarisation. This indicates that the anomaly is from an electron resonance. However, the Alfvén wave interference pattern is a factor of three stronger with hole polarisation. This is surprising because the Alfvén wave propagation is in a plasma with an equal number of electrons and holes which are expected to oscillate in phase with equal amplitudes because there is a zero, first-order Hall effect. However, it should be borne in mind that the real normal modes of propagation are circularly polarised even in a compensated plasma. The threshold for propagation occurs in one case at the cyclotron resonance condition for holes, and in the other at the electron cyclotron resonance. Since holes are lighter, the propagating wave acquires a higher amplitude for the hole polarisation at a given magnetic field.

The normal modes of propagation are circularly polarised as demonstrated in this experiment. The linear polarisation which is associated with Alfvén waves is an approximation that improves as the magnetic field increases above the cyclotron resonance condition of the heavier carrier. The dispersion in this approximation is described by the effective mass density in equation (4). Since it agrees with the measured value, it is clear that the dispersion of the propagating wave is given quite well by the Alfvén wave approximation even when the amplitude of one mode is affected by the proximity of the cyclotron resonance to the magnetic field.

The scattering rate depends, according to equation (5), on the DC conductivity, which undergoes changes from the Shubnikov–de Haas effect when a Landau level coincides with the Fermi energy. The magnetic fields for this condition determined by the spin-split minima in the magnetoresistance are 7.40 and 6.60 T for $n = 1$ electrons and 3.663

and 3.412 T for $n = 1$ holes (Wollam 1970). In figure 1, there is a marked decrease in the amplitude at the condition for holes but not for electrons. Thus, the amplitude is influenced by hole scattering. This is consistent with the observation that the component of Alfvén wave with hole polarisation has a larger amplitude.

The Alfvén wave amplitude transmitted through the sample is (Furdyna and Krauss 1971)

$$E_t = (4B/cM)\exp(-M\nu_{eff}d/2B)\exp[i(M\omega d/B)E_0]$$

from which ν_{eff} can be determined by plotting $\ln(E_t/B)$ versus B^{-1}. The slope of this plot for the data of figure 1 yields $\nu_{eff} = (1.3 \pm 0.3) \times 10^{10}\ s^{-1}$. This is for single-crystal graphite and is a factor of two smaller than the effective scattering rate for pyrolytic graphite derived by Furdyna and Krauss. Thus the scattering time is a factor of two larger in single-crystal graphite.

4. Conclusions

Alfvén wave propagation is evident in single-crystal graphite in magnetic fields up to 8.5 T at wavelengths between 392.5 μm and 512.5 μm. It is not observable in HOPG graphite at far-infrared wavelengths and in single-crystal graphite at 118.8 μm. The mass density describing the wave velocity is in agreement with that predicted from the properties of graphite. The propagation is sensitive to the sense of circular polarisation of the infrared and exists for hole polarisation. The amplitude of the Alfvén wave is reduced when a hole Landau level coincides with the Fermi surface. The effective scattering rate for Alfvén wave propagation is a factor of two smaller in single-crystal graphite than it is in pyrolytic graphite at a frequency of 35 GHz.

Acknowledgments

The technical design and improvement of the laser by C Verge and preliminary experiments by S Shier made this experiment possible. The research was supported by the Natural Sciences and Engineering Research Council of Canada.

References

Buchsbaum S J and Galt J K 1961 *Phys. Fluids* **4** 1514
Doezema R E, Datars W R, Schaber H and Van Schyndel A 1979 *Phys. Rev.* **19** 4224
Furdyna J K and Krauss A R 1971 *J. Phys. Chem. Solids* (suppl. 1) **32** 165
Isaacson R T and Williams G A 1969 *Phys. Rev.* **185** 682
McClure J W 1958 *Phys. Rev.* **112** 715
Palik E D and Furdyna J K 1970 *Rep. Prog. Phys.* **33** 1193
Schaber H and Doezema R E 1978 *Infrared Phys.* **18** 247
Soule D E, McClure J W and Smith L B 1964 *Phys. Rev.* **134** A453
Surma M, Furdyna J K and Praddaude C 1964 *Phys. Rev. Lett.* **13** 710
Wollam J A 1970 *Phys. Rev. Lett.* **25** 810